CHAPTER 3

METHODOLOGY

This chapter provides a detailed overview of the materials and methodology employed in this study for registering Computed Tomography (CT), Magnetic Resonance Imaging (MRI), and Ultrasound (US) images of cardiovascular patients. The registration process consists of three significant stages: temporal registration development, spatial registration development, and validation of the trimodality image registration scheme.

3.1 Image and Data Acquisition

CT, MRI, and US image data of simulation prior to radiation therapy from twenty patients diagnosed with Cardiovascular Diseases (CVD) were recruited in this study to approve patients' consent to undergo trimodality imaging. The Medical Research and Ethics Committee (MREC), Ministry of Health (MOH) Malaysia, approved the review and consent procedure. Other than that, permission from the Director of Hospital Serdang, Selangor, was obtained before the research. All data were collected retrospectively under the standard clinical acquisition protocol. The 20 patients were diagnosed with CVD between 2015 and 2020, respectively. Among the 20 patients with CVD, a subset had aortic valve diseases. Consequently, the letter of approval for ethics is annexed to Appendix A.

Section 3.1.1 presents an overview of the many imaging techniques used in this investigation. Finally, Section 3.1.2 provides data on patient characteristics acquired while recruiting participants for this research.

3.1.1 Image Acquisition

The CT, MRI, and US data sets were obtained at Hospital Serdang in Selangor, Malaysia. The MREC granted ethical approval. The hospital archiving systems provided the images as anonymized Digital Imaging and Communications in Medicine (DICOM) files. A 64-slide dual-source CT scanner Siemens Somatom Definition Flash captured CT images during image acquisition in the supine position. The total number of slices was 128, with a slice thickness of 1 mm – 5 mm and rotation scan times of 0.33, 0.5, and 1 s, respectively. Note that the matrix had 512 × 512 pixels.

MRI data were obtained retrospectively with a Siemens Magnetom Symphony scanner and were provided from the hospital archiving systems as anonymized DICOM files. The slice thickness was 8 mm, with a scanning interval of 25%. The Field of View (FOV) was 230 × 230 mm^2, and the matrix size referred to the patient's image.

The US data sets were also retrospectively gathered from the same patients and delivered as DICOM from hospital archival systems anonymously. US of the two-dimensional time series was carried out with the Cardiology US System (Philips Epic 7C). The image obtained includes the "Mercedes Benz" short axis, an indicator for the aortic valve plane. It covers 4 to 5 cardiac cycles with a spatial resolution of 0.3 to 0.3 mm.

3.1.2 Patient Characteristics Data

The data in Table 3.1 presents the characteristics of the 20 recruited patients included in the study conducted at Hospital Serdang, Selangor, Malaysia. This study utilized three different modalities for analysis. The characteristics of the patients, such as their age and gender, are outlined in the table.

As previously stated in Chapter 2, it has been observed that a significant number of deaths caused by CVD occur in individuals below the age of 70. This age group constitutes 46% of the total deaths, indicating that a considerable portion of the population affected by CVD is in the prime years of their lives. Furthermore, it is worth noting that 79% of the burden of the disease is concentrated within this particular age group (Yuyun et al., 2020).

Table 3.1: Patient Characteristics Who Were Recruited for This Research

Patient #	Gender	Age
1	F	37
2	M	47
3	M	41
4	M	18
5	M	48
6	M	40
7	M	63
8	M	53
9	M	33
10	F	46
11	M	67
12	F	24
13	M	29
14	M	31
15	F	24
16	F	56
17	M	34
18	M	73
19	F	52
20	F	32

F = Female, M = Male

3.2 Description of Methodology

The investigation of trimodality image registration for CVD comprises three main steps: the development of temporal registration, the development of spatial registration, and the validation of the trimodality image registration scheme. This study implements the rigid-body registrations of US + CT and US + MRI separately using MATLAB's image registration tool (vR2020b, MathWorks, Natick, USA). By utilizing the common

data measure, the software aligns the secondary image sets of CT and MRI with the primary image set of the US. Consequently, these aligned secondary image sets are incorporated into an in-house developed software for trimodality image registration.

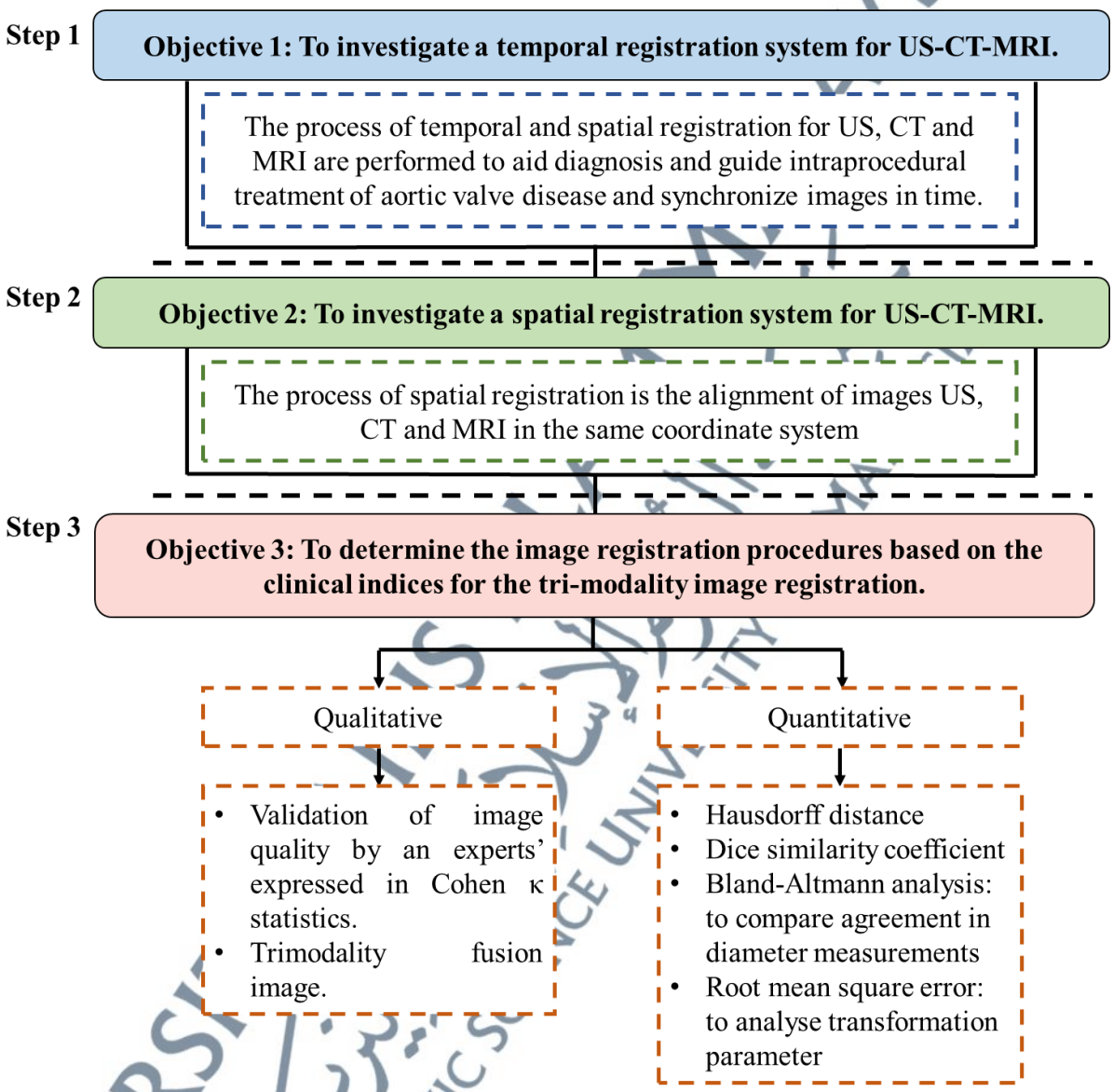

Figure 3.1: Flowchart Overall Workflow of The Research Framework

This research methodology is divided into three major steps to achieve the research objectives, demonstrated in the flowchart in Figure 3.1. This flowchart describes an overall workflow that will be conducted in general. The images of individual modalities are acquired at different times. Thus, in the first stage, the US-

CT-MRI will be aligned and synchronized in time. In the second stage, the spatial registration algorithm will utilize a mutual information scheme combining a rigid or nonrigid geometrical transformation to align the modalities in the same coordinate system or spatial location. Finally, the trimodality image registration accuracy and the visual output quality will be validated qualitatively and quantitatively in the validation stage. The entire suggested registration procedure for this research is illustrated in Figure 3.2, and the following sections provide a more in-depth analysis of each stage.

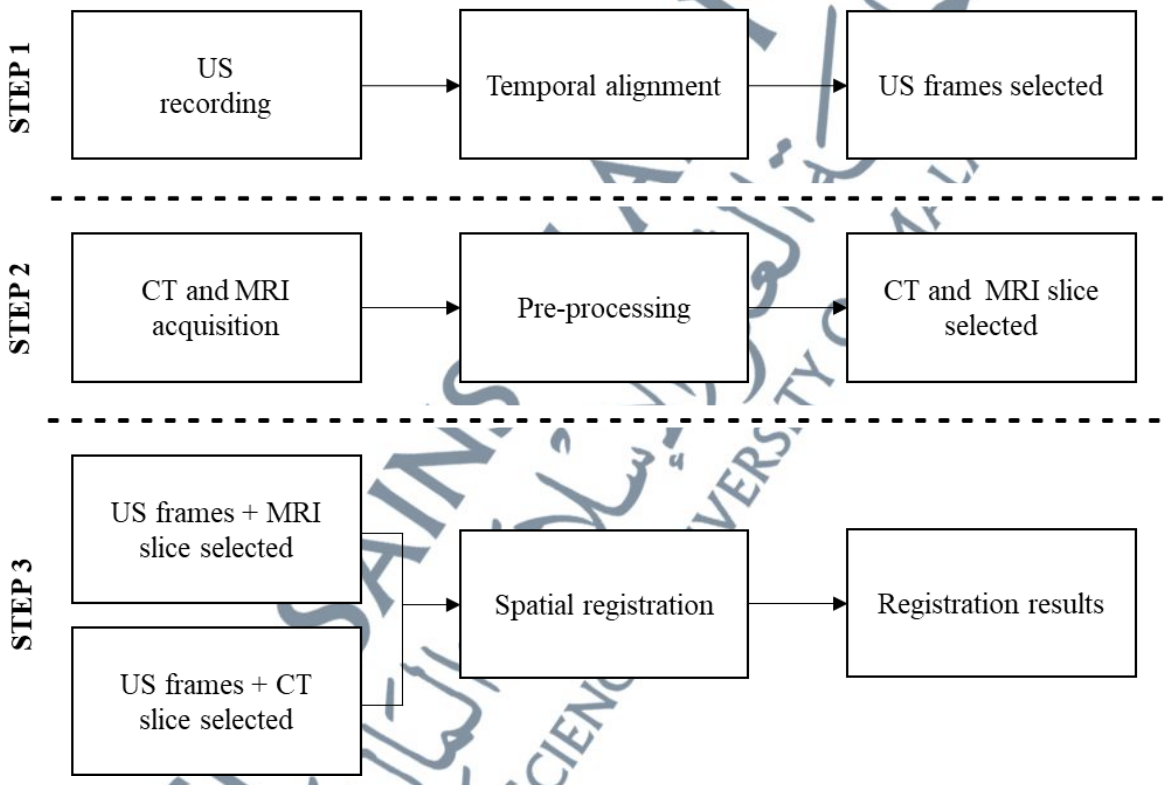

Figure 3.2: Registration Procedure

3.3 Temporal Registration

In order to achieve Objective 1, Step 1 will be employed. The investigation of the temporal registration system follows the previous work reported by (Perperidis et al., 2004 & Khalil et al., 2016). To register two or more images spatially, it is first necessary to temporally align them to discover corresponding frames due to differences in

temporal sampling. Using the method of Perperidis et al. (2005), we adjust the temporal and spatial components independently to achieve this goal. Through temporal registration, we check to see if both sequences have the same number of frames and do this by locating critical temporal frames. To complete the enhanced sequence, we interpolate new frames into the originals at strategic points.

In Step 1, the temporal registration was performed to synchronize US + CT and US + MRI in time. These modalities produce images with various sampling latencies and temporal resolutions. Other than that, the series of US images in the corresponding state or most similar to the diastole phase of CT and MRI acquisition of cardiac will be extracted from US videos. To achieve an excellent temporal alignment, both sequences of US frames, plus CT or MRI frames, must contain an equal number of frames for detecting key temporal frames. The interpolated sequence frames between keyframes will be generated to produce the augmented sequence.

This study used time stamping to achieve temporal registration of CT, MRI, and US imaging modalities using the Electrocardiogram (ECG) gating signal obtained simultaneously during US imaging. The ECG signal's R peaks are automatically identified based on the signal amplitude (Ghodsizad et al., 2021). The ECG signal underwent linear interpolation within the R-R interval, as depicted in Figure 3.3, to identify US images corresponding to similar heart phases as the preoperative cardiac CT and MRI volume. For spatial registration, three frames were selected between 40% and 70% of the interval. The time delay recorded in the CT and MRI header file was utilized to calculate the period, which closely aligned with the end-diastolic phase of the heart cycle.

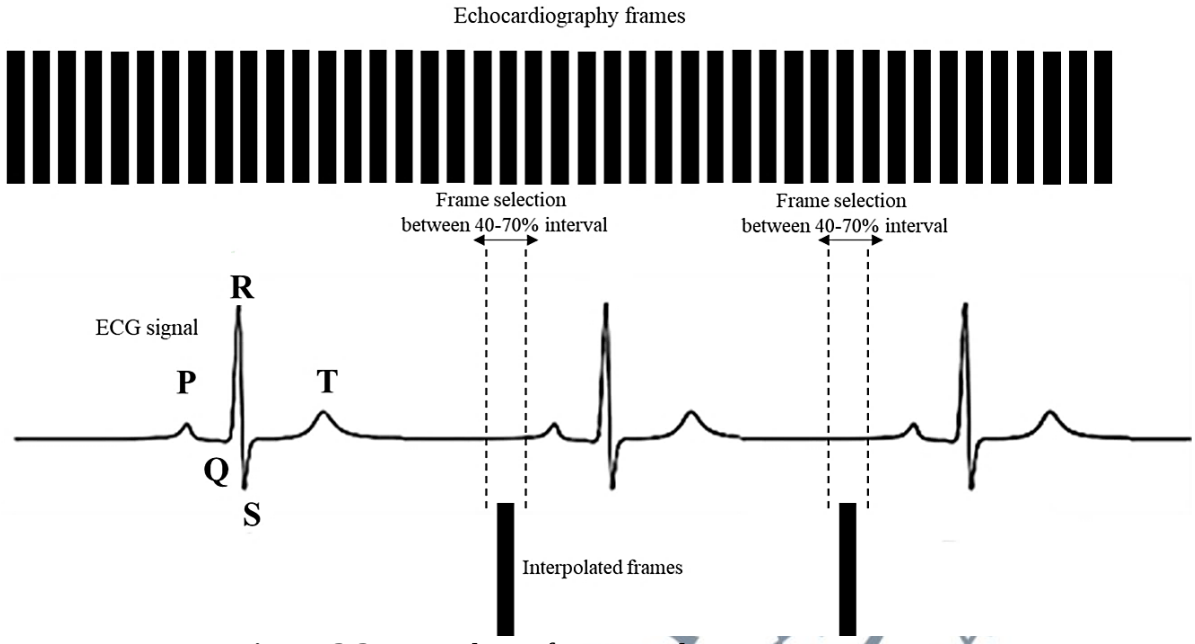

Figure 3.3: Procedure of Temporal Registration

3.4 Spatial registration

Step 2 will be applied to achieve Objective 2, which investigates a spatial registration system for US, CT, and MRI. A rigid intensity registration scheme from 2D to 3D will be used in this step. It will use mutual knowledge as a search metric of similarity and pattern as its underlying optimizer to develop the spatial registration of the 2D US frame with the corresponding CT and MRI volumes of preoperative cardiac. In addition, the US image from Step 1 will be used to explore the best compatible plane for both the cardiac CT and MRI planes by spatially manipulating the proximity of the cardiac CT and MRI volume. Figure 3.4 illustrates this study's overall proposed framework for spatial registration, with the specifics of each step addressed in the following paragraph.

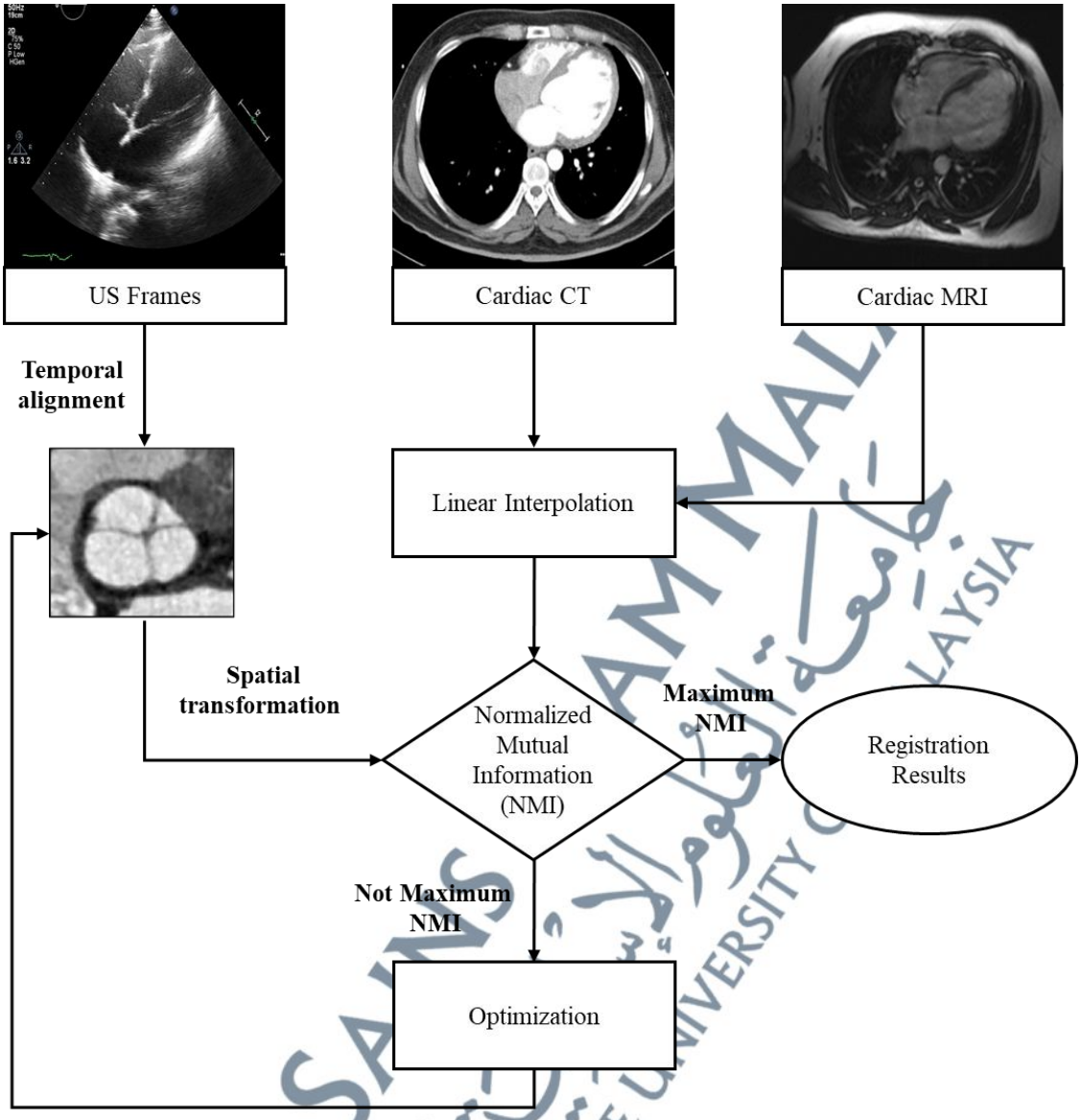

Figure 3.4: Overall Spatial Registration Workflow

3.4.1 Spatial transformation

In the spatial transformation, the search for the optimal matching plane in CT and MRI begins by determining and positioning the US image seed. The placement of the seed position for the registration of cardiac CT and MRI depends on the selected views. This analysis selects the "Mercedes Benz" view as the seed position, as illustrated in Figure 3.5. The expert estimates and provides the orientation and location of the valve

plane in the seed position, considering the patient's body's three-dimensional (3D) axes in preprocedural planning for the CT and MRI volume (Rahimi et al., 2021).

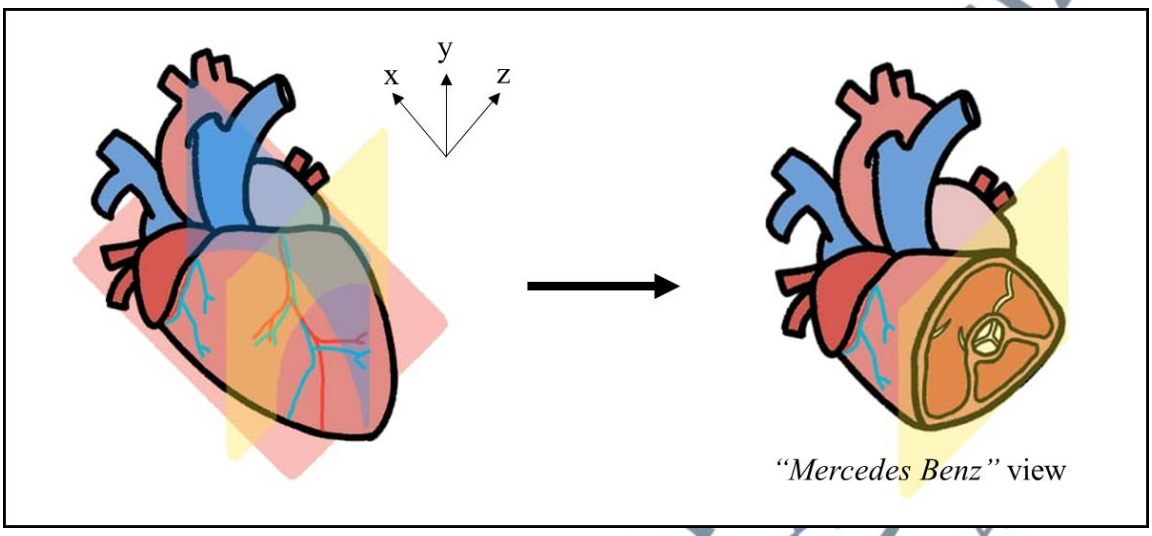

Figure 3.5: "Mercedes Benz" Seed Plan View Sketching Initiated The Registration Search

The two-dimensional (2D) planar US images were subjected to a rigid spatial transformation, denoted by the letter T, which contained 8 degrees of freedom and consisted of the following components:

1. 3D translation (t_x, t_y, and t_z)
2. 3D rotation (r_x, r_y, and r_z)
3. 2D scaling (s_x and s_y, i.e., along both axes of the image plane).

The transformation matrix and its constituent parts are displayed in Equations 3.1-3.3. They were utilized for this research, where i, j, and k are the coordinates of the picture that is being input, i', j', and k' are the coordinates that have been transformed, and α, β, and γ are the rotation angles about the x, y, and z axes, respectively.

$$\begin{bmatrix} i' \\ j' \\ k' \\ 1 \end{bmatrix} = T \times \begin{bmatrix} i \\ j \\ k \\ 1 \end{bmatrix}, \quad (3.1)$$

$$T = scaling \times rotation \times translation,$$

(3.2)

$$T = \begin{bmatrix} s_x & 0 & 0 & 0 \\ 0 & s_y & 0 & 0 \\ 0 & 0 & 1 & 0 \\ 0 & 0 & 0 & 1 \end{bmatrix} \times \begin{bmatrix} 1 & 0 & 0 & 0 \\ 0 & \cos\alpha & -\sin\alpha & 0 \\ 0 & \sin\alpha & \cos\alpha & 0 \\ 0 & 0 & 0 & 1 \end{bmatrix} \times \begin{bmatrix} \cos\beta & 0 & -\sin\beta & 0 \\ 0 & 1 & 0 & 0 \\ \sin\beta & 0 & \cos\beta & 0 \\ 0 & 0 & 0 & 1 \end{bmatrix} \times \begin{bmatrix} \cos\gamma & -\sin\gamma & 0 & 0 \\ \sin\gamma & \cos\gamma & 0 & 0 \\ 0 & 0 & 1 & 0 \\ 0 & 0 & 0 & 1 \end{bmatrix} \times \begin{bmatrix} 1 & 0 & 0 & 0 \\ 0 & 1 & 0 & 0 \\ 0 & 0 & 1 & 0 \\ t_x & t_y & t_z & 1 \end{bmatrix}.$$

(3.3)

3.4.2 Linear Interpolation

Subsequently, the most common interpolation technique, linear interpolation, follows the previous work mentioned by (Maes et al., 1997; Zhu & Cochoff, 2002; Xie et al., 2003; Khalil et al., 2017a). This technique is used to sample 2D CT and MRI planes with identical size and spatial position as the US image of both cardiac CT and MRI volumes. First, it has been converting points from one image to the next. Consequently, Normalized Mutual Information (NMI) was determined as the optimal alignment of the best matching 2D CT and MRI planes.

3.4.3 Normalized Mutual Information

The NMI originates from Shannon's (1948) classic and profoundly influential work. The mutual information within discrete random variables X, Y, and Z, also related to transformation (Equations 3.4 and 3.5), is described as:

$$I(X;Y|Z) = H(X) + H(Y) + H(Z) - H(Y|Z),$$

(3.4)

$$I(X;Y|Z) = \sum_{i=1}^{I}\sum_{j=1}^{J}\sum_{k=1}^{K} p(x_i, y_j, z_k) \log\left(\frac{p(x_i, y_j, z_k)p(z_k)}{p(x_i, z_k)p(y_j, z_k)}\right), \quad (3.5)$$

where *H(X)*, *H(Y)*, and *H(Z)* are the Shannon-Weiner entropies of cardiac CT and MRI, and US images, respectively. Meanwhile, $p(x_i, y_j, z_k)$, $p(z_k)$, $p(x_i, z_k)$, and $p(y_j, z_k)$ denote the joint and marginal probabilities of three images that can be estimated from the normalized joint histogram. Assuming X is the 2D interpolated CT plane, Y is the 2D interpolated MRI plane, and Z is the US image, the normalized mutual information metric NMI $(X; Y|Z)$ is presented by Equation 3.6:

$$NMI(X;Y|Z) = \frac{1}{n}\sum_{k=1}^{n} \frac{H(X) + H(Y) + H(Z_K)}{H(Y|Z_K)}, \quad (3.6)$$

where n denotes the number of frames from the US used in the registration process.

To compensate for the variation in magnitude order between parameters, all transformation parameters will be scaled to the range of -1 to 1 (except for 0 to 1 due to scaling) during the optimization phase. It improves the conversion speed and performance accuracy. Parallel processing has been used to test the objective functions, and the optimizer has been iterated up to a sufficiently small search step. Consequently, the convergence to a maximum NMI will be obtained. Both cardiac CT and MRI volumes will be optimized to produce a matching 2D CT and MRI image using the optimized transformation found. The images will then be merged to create a composite image with a US image as surgical guidance.

3.4.4 Optimization

In order to determine the optimal parameters for spatial transformation that maximize the NMI measure of overlap between pixel intensities in the image, an iterative Generalized Pattern Search (GPS) algorithm was applied to the image registration problem. The GPS algorithm belongs to a class of numerical optimization techniques that eliminate the need to consider the gradient of the objective function. It makes it particularly suitable for functions like mutual information, which cannot be divided into multiple distinct functions in their conventional form. Moreover, the GPS algorithm samples points in a predetermined pattern around the seed position determined by CT and MRI prior to the procedure (Zhang et al., 2021).

To address the varying scales of parameters and improve convergence speed and accuracy, we normalized all transformation parameters to a range of -1 to 1 (excluding scaling from 0 to 1) during the optimization process. Other than that, parallel processing was utilized to evaluate the objective functions, and the optimizer iterated until the search step became small enough to converge toward the highest NMI value. The resulting best transformation of the cardiac CT and MRI volume provided an exact match with a 2D CT and MRI planar image. Combined with US images, this image can be merged to create a composite image for surgical navigation.

3.5 Verification of Registration Accuracy

To achieve Objective 3, to establish image registration validation procedures using clinical indices for trimodality image registration, both qualitative and quantitative assessments.

3.5.1 Qualitative Assessment

The registration of the suggested technique will be measured using the manual registration of the gold standard. Validation occurs in twenty patients on the "Mercedes Benz" short axis view.

1. Articulating The Alignment To The Gold Standard

The experts were required to complete the manual registration process, which consisted of manually changing the transformation parameters. In order to accomplish this, the transformation parameters are approximated using the expert's understanding of the orientation of the US plane with regard to the heart's position within the patient's body. Aligning the US with the cardiac CT and MRI was done using rotation, translation, and scaling in the x, y, and z directions, and the results were regarded as the gold standard. Note that this method has been demonstrated to have a localization inaccuracy of less than one millimeter.

2. The Image Quality of Cardiac CT and MRI

The experts evaluated the registered image according to the image quality of the interpolated CT and MRI images and rated the images with a score from 1 to 4 qualitatively. The interobserver image quality agreement has been represented as the Cohen κ statistics by (Galton, 1893) for cardiac structure morphology on CT and MRI. The following is the summary of the score:

- The rate of score 1 is expressed as outstanding image quality. The picture demonstrates excellent clarity and distinction of the anatomical aspects of the heart structure important to treat heart valves by surgery. It is also shown that the structure viewed in both images is very comparable to the US image.

- The rate of score 2 is expressed as good image quality. The picture provides a good insight into the related valve treatment anatomical details. It is also presented that the structure viewed in the US images is similar.
- The rate of score 3 is expressed as weak yet still diagnostic. The picture shows the anatomic features being poorly visible. As seen in the US, the plane tends to be slightly off the standard valve.
- The rate of score 4 is expressed as bad. The image demonstrates the quality of nondiagnostic images, and no anatomical structures and roots can be delineated. The plane is entirely off and distinct from the appearance of the US.

3.5.2 Quantitative Assessment

In order to determine the registration accuracy quantitatively, the experts utilized US imaging to segment the aortic valve. They selected the CT and MRI planes that closely matched the anatomical structures for comparison. The Dice Similarity Coefficient (DSC) and Hausdorff Distance (HD) metrics were calculated on the contoured region to measure the degree of overlap and the maximum distance between the registered images, respectively. Besides, Bland-Altman analysis was performed to evaluate the agreement in diameter measurements obtained from two different registration methods: the automated trimodality registration system and the manual gold standard registration. The root-mean-square error was computed to assess the quality of the transformation settings. Other than that, these quantitative analyses are described in detail in the subsequent sections.

1. Manual Segmentation

Accurately assessing the aorta's mechanical and hemodynamic properties requires segmentation, a crucial part of the process. The expert conducted manual segmentation on the CT and MRI images produced due to manual and automatic registration, in addition to the US images. The contouring of the aortic valve cross section can be seen in the views of the "Mercedes Benz" sign. These views are vital for making a diagnosis, particularly regarding aortic valve dysfunction.

2. Dice Similarity Coefficient

DSC is the evaluation of the spatial overlap between two contoured Regions of Interest (ROI), following the previous work reported by Zou (2004) and Khalil (2017b). This study assesses the spatial overlap in the most accurate complement between US + CT and US + MRI. This assessment is sensitive to both the size and position of the contoured ROI and is represented as:

$$DSC = \frac{1}{n}\sum_{j=1}^{n}\frac{2(R_A \cap R_{B_j})}{R_A + R_{B_j}} \quad (3.7)$$

In Equation 3.7, both the US + CT and US + MRI contoured ROI will be interpreted as R_A and R_B, respectively. The US number used for registration shall be represented as n. The indication for DSC representing spatial overlap and reproducibility that ranges from 0 to 1 are presented in Table 3.2.

Table 3.2: The DSC Indications Represent Spatial Overlap and Reproducibility

Spatial Overlap of Two Contoured ROI (A and B)	DSC Indications
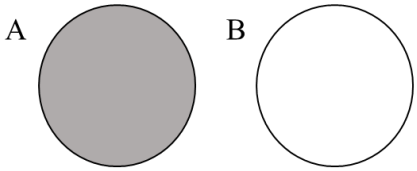	No overlapping : DSC = 0
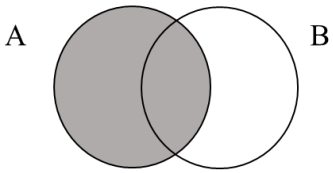	Partial overlap: $0 \leq DSC \leq 1$
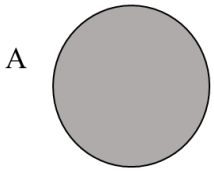	Perfect overlap: DSC = 1

3. Hausdorff Distance

HD is a widely used measure for evaluating the performance of medical image segmentation techniques. Similar to previous studies conducted by Khalil (2017b) and Karimi & Salcudean (2020), this technique will be employed to quantify the spatial distance between two ROIs based on their contour points. The HD is defined as follows:

$$H(A,B) = \max\big(h(A,B), H(B,A)\big), \tag{3.8}$$

where

$$h(A,B) = \max_{a\in A} \min_{b\in B} \|a-b\|. \tag{3.9}$$

In Equations 3.8 and 3.9, the function $h(A,B)$ is described as the directed HD from A to B, in which A and B are two collections of contour points in the US + CT for US + MRI, respectively. It identifies the mutual proximity between two ROIs by

designating the maximal distance between any point of ROI to another ROI. Note that HD is one of the most informative and valuable criteria, which is becoming an indicator of the most massive segmentation error, mainly in this study.

When comparing three modalities, the DSC and HD metrics evaluate how similar or different the aortic is in area and shape. This indirectly measures the registration's accuracy. Although the clinical goal is to merge 2D US with interpolated planes of CT and MRI, these 2D measures of aortic valves are considered suitable measurements for testing the registration accuracy of the proposed technique.

4. Bland-Altman Analysis

The Bland-Altman analysis was proposed by Martin Bland and Altman (1986). This analysis compares the agreement derived from two distinct mechanisms in diameter measurements. The aortic diameter was determined from both registered CT and MRI planes automatically and manually. Apart from that, the annulus diameter is calculated for the aortic valve by the circumcircle diameter of the annulus valve. It is due to the noncircular shape of the aortic valve in the signpost view “Mercedes Benz”. Using Bland-Altman plots, we analyzed the consistency of diameter values from two distinct registration methods to see how closely they aligned.

5. Root Mean Square Error

In order to perform a quantitative analysis of the transformation parameters, the Root Mean Square Error (RMSE) was calculated to assess the similarities and differences between the manual and automatic registration processes for each parameter. Equation 3.10 defines the specific calculation for this metric.

$$RMSE = \sqrt{\frac{1}{N}\sum_{i=1}^{N}(t_m - t_a)^2}. \quad (3.10)$$

In Equation 3.10, t_m is a parameter for transformation (which might be either translation, rotation, or scaling) acquired from the manual registration performed by an expert. Subsequently, the corresponding transformation parameter that the suggested algorithm has produced is denoted by the letter t_a.